Electronic Supplementary Material (ESI) for ChemComm.

Directing GDNF-Mediated Neuronal Signaling with Proactively Programmable Cell-Surface Saccharide-Free Glycosaminoglycan Mimetics

Shuting Cai, Daniel H. Lukamto, Jerry K. C. Toh, Roland G. Huber, Peter J. Bond, Joo-Eun Jee, Teck Chuan Lim, Pei Liu, Liwei Chen, Qianqian Vicky Qu, Su Seong Lee and Song-Gil Lee*

Electronic supplementary information

(Materials and methods, Fig. S1-S22, Table S1, Supplementary References)

General methods

Unless otherwise stated, reactions were performed using anhydrous solvents and in flame-dried glassware under argon atmosphere. All commercial reagents were used as received unless otherwise stated. 1,2-Dipalmitoyl-*sn*-glycero-3-phosphoethanolamine-N-(succinyl) (sodium salt) (catalogue number 870225P) was purchased from Avanti Polar Lipids, Inc. EZ-link NHS-PEG12-Biotin (catalogue number 21313) and EZ-Link Hydrazide-PEG4-Biotin (catalogue number 21360) were purchased from Thermo Scientific. Heparan Sulfate polysaccharides were purchased from Iduron (catalogue number GAG-HSIII) with an average molecular weight of 9,000 dalton. P-selectin (catalogue number 737-PS) and L-selectin (catalogue number 576-LS) were purchased from R&D Systems. Recombinant human β-nerve growth factor (NGF) (catalogue number 450-01) were purchased from PeproTech. Thin layer chromatography (TLC) was performed using E. Merck silica gel 60 F254 precoated plates (0.25 mm) and visualization of the developed chromatogram was performed by UV, cerium ammonium molybdate or ninhydrin stain as necessary. Merck silica gel 60 (particle size 0.040 - 0.063 mm) was used for flash chromatography. Peptide purification was conducted on Gilson HPLC GX-271 System equipped with a reverse phase Kromasil® 100-5-C18 column (21.2 x 250 mm) or or a normal phase XBridge™ Prep HILIC column, 5 μm (10 x 100 mm). Gel filtration chromatography (Sephadex G-15 or LH-20 ultrafine: GE Healthcare) was used for the purification of polyproline-based glycosaminoglycan mimetics (PGMs).

^{1}H NMR spectra were recorded on a Bruker AVIII 400 (400 MHz) spectrometer and are reported in parts per million (δ) relative to D_2O (4.79 ppm). Data for the ^{1}H NMR spectra are reported as follows: chemical shift (δ ppm), multiplicity (s = singlet, brs =

broad singlet, t = triplet, m = multiplet), coupling constant in Hz, and integration. Mass spectra were obtained from Waters SQD Quadrupole Mass Spectrometer equipped with Waters Acquity™ Ultra Performance Liquid Chromatography (column: Waters Acquity UPLC® BEH C18 1.7 µm (1.0 x 150 mm) or Waters Acquity UPLC® BEH HILIC 1.7 µm (2.1 x 100 mm)) and were recorded in m/z. HPLC conditions for C18 column were: 1) 5% A over 0.5 min; 2) 5-60% A over 5.5 min; 3) 60-80% A over 0.5 min and; 4) 80% A over 1.5 min (where A: 99.9% CH_3CN / 0.1%TFA, B: 90% H_2O / 9.9% CH_3CN / 0.1% TFA, %A + %B = 100%, flow rate = 0.3 mL/min). HPLC conditions for HILIC column were: 1) 25-100% A over 5.5 min; 2) 100% A over 2.0 min (where A: 99.9% CH_3CN / 0.1%TFA, B: 90% H_2O / 9.9% CH_3CN / 0.1% TFA, %A + %B = 100%, flow rate = 0.3 mL/min). FT-IR spectra were collected using Perkin-Elmer Spectrum 100 and are reported in terms of wavenumber (cm^{-1}).

Abbreviation

DIPEA	N,N-Diisopropylethylamine
TBTU	N,N,N′,N′-Tetramethyl-O-(benzotriazol-1-yl)uranium tetrafluoroborate
HOBt	Hydroxybenzotriazole
TFA	Trifluoroacetic acid
TBTA	Tris[1-benzyl-1H-1,2,3-triazol-4-yl)methyl]amine
PEG	Polyethylene glycol
PyBOP	Benzotriazol-1-yl-oxytripyrrolidinophosphonium hexafluorophosphate
DPPE-succinyl-OH sodium salt	1,2-dipalmitoyl-sn-glycero-3-phosphoethanolamine-N-(succinyl) (sodium salt)

General procedure for the synthesis of PGM precursors.

All PGM precursors were prepared *via* standard Boc chemistry in the solution phase as reported previously.[1] Briefly, to a solution of Boc-Peptide(1)-OH (1.0 equiv.) in DMF were added H-Peptide(2)-OCH_3 (1.1 equiv.), TBTU (1.1 equiv.) and DIPEA (5.0 equiv.) (final concentration: 0.1 M). The mixture was stirred at room temperature until the reaction was completed. After the completion, the solvent was removed *in vacuo* to afford a yellow solid. Purification of this solid by either flash column chromatography on silica or reverse phase HPLC afforded Boc-Peptide(1)-Peptide(2)-OCH_3. To deprotect methyl ester group, aq. NaOH (2.0 equiv.) was added to a solution of Boc-Peptide(1)-Peptide(2)-OCH_3 (1.0 equiv.) in THF/MeOH (1:1, final concentration was adjusted to 0.05M) and sonicated for 5 min. At this time, the same volume of CH_2Cl_2 was added and the reaction was stirred for additional 2 h. It was then neutralized with Amberlyst IR-120 resin, filtered and evaporated *in vacuo* to afford Boc-Peptide(1)-Peptide(2)-OH quantitatively. To deprotect Boc group, Boc-Peptide(1)-Peptide(2)-OCH_3 was dissolved in CH_2Cl_2/TFA (1:1) at 0 °C and stirred for 2 h. After the completion, the solvent was removed by blowing a slow stream of nitrogen gas and then diethyl ether was added to give H-Peptide(1)-Peptide(2)-OCH_3 quantitatively as a white precipitate. Purification of crude compounds by reverse phase HPLC afforded desired final PGM precursors as a white solid.

Procedure for the synthesis of Boc-$\{Z_A\}_{12}$-B.

To a solution of Boc-$\{Z_A\}_{12}$ -OH (1.0 equiv.) in DMSO (final concentration: 0.1 M) were added EZ-Link Hydrazide-PEG4-Biotin (1.0 equiv., Thermo Scientific), TBTU (1.1

equiv.) and DIPEA (5.0 equiv.). The reaction mixture was stirred at room temperature for an additional 2 hr. Upon completion, the solvent was removed *in vacuo* to afford yellow oil. Purification by size exclusion chromatography (Sephadex LH-20 with MeOH/CH_2Cl_2 (1:1)) afforded **Boc-{Z_A}$_{12}$-B** as a white solid that was directly used for the next step without further purification (Fig. S1B, ESI†).

General procedure for the synthesis of B-Azidopolyproline-OCH_3.

To a solution of H-Azidopolyproline-OCH_3 (1.0 equiv.) in DMSO (final concentration was adjusted to 0.1M) were added EZ-link NHS-PEG12-Biotin (1.2 equiv., Thermo Scientific: catalogue number 870225P) and DIPEA (5.0 equiv.), and stirred overnight at room temperature. After the completion, the solvent was removed *in vacuo* to afford a yellow sticky solid. Purification of this solid by reverse phase HPLC afforded B-azidopolyproline-OCH_3 (Fig S1A and Fig S2–S4, ESI†).

Procedure for the synthesis of DPPE-{Z_A}$_{12}$-B.

To a solution of H-{Z_A}$_{12}$-B (1.0 equiv.) in anhydrous DMF/CH_2Cl_2/THF (2:1:1, final concentration: 0.1 M) were added DPPE-succinyl-OH sodium salt (1.0 equiv.), PyBOP (2.0 equiv.), HOBt (2.0 equiv.), and DIPEA (5.0 equiv.), and stirred at room temperature for 3 days under argon atmosphere. Upon completion, the solvent was removed *in vacuo* to afford yellow oil. Purification by HPLC equipped with HPLC XBridge™ Prep HILIC column afforded **DPPE-{Z_A}$_{12}$-B** as a white solid (Fig S1B, Fig S11 and Fig S14, ESI†).

Procedure for the synthesis of DPPE-$\{Z_A\}_{12}$.

To a solution of H_2N-$\{Z_A\}_{12}$ (1.0 equiv.) in anhydrous DMF/CH_2Cl_2/THF (2:1:1, 0.1 M of final concentration) were added DPPE-succinyl-OH sodium salt (1.0 equiv.), PyBOP (2.0 equiv.), HOBt (2.0 equiv.) and DIPEA (5.0 equiv.). The reaction mixture was stirred at room temperature for 3 days under argon atmosphere. Upon completion, the solvent was removed *in vacuo* to afford yellow oil. Purification by HPLC equipped with HPLC XBridge™ Prep HILIC column afforded **DPPE-$\{Z_A\}_{12}$** (Fig S1C, Fig S12 and Fig S14, ESI†).

Procedure for the synthesis of DPPE-12-$\{Z_A\}_{12}$.

To a solution of H_2N-PEG12-$\{Z_A\}_{12}$ (1.0 equiv.) in anhydrous DMF/CH_2Cl_2/THF (2:1:1, 0.1M of final concentration) were added DPPE-succinyl-OH sodium salt (1.0 equiv.), PyBOP (2.0 equiv.), HOBt (2.0 equiv.), and DIPEA (5.0 equiv.). The reaction mixture was stirred at room temperature for 3 days under argon atmosphere. Upon completion, the solvent was removed *in vacuo* to afford yellow sticky oil. Purification of this oil was carried out by precipitating in acetonitrile (5 mL x 2) and methanol (5 mL x 2) to afford **DPPE-12-$\{Z_A\}_{12}$** as a white solid (all excess reagents and impurities were successfully removed) (Fig S1D, Fig S13 and Fig S14, ESI†).

General procedure for the click reaction.

Pent-4-yne-1,2-diyl bis(sulfate) **2** (1.3 equiv. per azide), PGM precursor (1.0 equiv.), and TBTA (0.3 equiv. per azide) were added into a vial. Under argon atmosphere, the mixture was dissolved in anhydrous DMSO (final concentration: 0.1 M) and copper (I) iodide

stock solution in DMSO (0.3 mol% per azide) and DIPEA (48.0 equiv.) were sequentially added. The reaction mixture was then stirred for 14 days at room temperature under argon atmosphere. After complete consumption of azide functionality, the solvent was removed with continuous nitrogen flow. The resulting mixture was dissolved in 200 μL of 4M aq. NaCl and purified by Sephadex G-15 column (100% H_2O). Upon lyophilization, the desired PGMs were afforded as a white solid.

The azide vibrational band (~2100 cm^{-1}) in FT-IR spectra was used to monitor the completion of the click reaction. FTIR was conducted using a Perkin Elmer FTIR Spectrum 100 between 4000 and 800 cm^{-1} at a spectral resolution of 4 cm^{-1} (4 scans per sample). Preparation of the FT-IR was done by placing the samples on a germanium stage. The samples were then pressed before the measurement. The disappearance of the azide vibrational band in the spectra of the PGMs indicated the completion of the coupling reactions (Fig S1E, Fig S4–S8 and Fig S15–S20, ESI†).

Circular dichroism (CD) analysis.

CD spectra were obtained using a Jasco-815 CD spectrometer equipped with a Peltier temperature controller (Jasco PTC-423S/15). 200 μM of sample solutions in 10 mM sodium phosphate-dibasic buffer (pH 7.0) were equilibrated at 4 °C for 24 h, followed by at room temperature for 1 hr before measurements. Spectra were recorded at 25 °C from 260 to 200 nm. Mean residue ellipticity [θ] was calculated as follows;

$$[\theta] = \theta/(10 \cdot N \cdot c \cdot l)$$

θ represents the ellipticity in millidegrees, N the number of amino acid residues, c the molar concentration in $mol \cdot L^{-1}$, and l the cell path length in cm (Fig. 1B).

Surface plasmon resonance.

SPR measurements were performed using a Biacore T100 system (GE Healthcare). The CM5 sensor chip was primed with HBS-EP+ buffer (10 mM HEPES pH 7.4, 150 mM NaCl, 3.4 mM EDTA, 0.005% P20, GE Healthcare) and was activated using the standard amine-coupling protocol (1:1 mixture of 0.4 M EDC and 0.1M NHS). 0.008 mg/ml of streptavidin solution in 10 mM sodium acetate buffer (Acetate 5.0, GE Healthcare) was conjugated and remaining activated groups were quenched with 1M ethanolamine solution (pH 8.5). The final amount of streptavidin covalently immobilized on the surface was typically 700 RU. Flow cell 1 (or 3) was used as a reference to subtract nonspecific binding, drift, and the bulk refractive index, while flow cell 2 (or 4) was further immobilized with GAG mimetic agents or natural polysaccharides. 5 nM of biotinylated PGMs (or heparan sulfate) were dissolved in HBS-EP+ buffer and were injected to flow cell 2 (or 4) at 30 μL/min until the baseline response increased by: (for GDNF) 10, 13, 15, 14 and 18 RU for **B-{Z}$_{12}$**, **B-{PZZ}$_{6}$**, **B-{PPZ}$_{12}$**, **B-{PPZZ}$_{6}$** and biotinylated heparan sulfate respectively; (for P-selectin and L-selectin) 24 RU for **B-{Z}$_{12}$**. Immobilized amount is normalized by the molecular weight. For a given affinity measurement, varying amount of protein solutions were successively injected into the flow cells for 240 seconds of contact time and 800 seconds of dissociation time using a flow rate of 50 μL/min at 25 °C. Flow cell was regenerated using 2.5 M $MgCl_2$ at 30 μL/min. Association (k_a) and dissociation (k_d) rate constants were calculated with a 1:1 binding model using Biacore evaluation software, and K_D values were calculated from the ratio of k_d to k_a. Kinetic parameters were obtained by fitting curves to a 1:1 Langmuir model with baseline correction.

Unbiased docking simulations.

Simulations of mimetic binding to GDNF were performed using the Amber molecular simulation package[2] using the Amber force field ff14SB.[3] Parameterization of proline residues modified with azide functional groups was performed as outlined in our earlier study Lim et al.[4] We extracted the structure of the GDNF dimer from the PDB (2V5E[5]), and removed the GDNF receptor family receptor α1 (GFRα1) contained in the structure. We created 200 independent starting geometries of $\mathbf{\{Z\}_{12}}$ by GDNF dimer at the center of a 7x7x7 nm^3 cubic box and randomly inserting the respective $\mathbf{\{Z\}_{12}}$ using the ′insert-molecules′ tool of the Gromacs suite[6] (Fig S10A, ESI†) as prescribed by the dynamic molecular docking (DMD) procedure.[7] Next, we ran simulations of 10 ns each for all 200 starting conformations using pmemd with implicit solvation,[8] using igb=5, mbondi2 radii[9] and a salt concentration of 0.15 M. Subsequently, we performed MM-GBSA calculations[10] on 200 frames from the final 1 ns of each binding simulation. The key interacting residues were identified by per-residue energy decomposition based on the criterion that average per-residue MM-GBSA energy derived from seven most favorable $\mathbf{\{Z\}_{12}}$/GDNF complexes (Fig S10B and S10C, ESI†) is lower than -5 kcal/mol.

General procedure for cell culture.

PC12 cells were maintained in T75 tissue culture flasks in RPMI 1640 medium (ATCC® 30-2001) supplemented with 10% heat-inactivated horse serum (HI-HS, Gibco 26050-088), 5% fetal bovine serum (FBS, Gibco 26170-043) and 1% penicillin/streptomycin (Gibco 15140-122). Stock cultures from liquid nitrogen were grown at 37 °C with 5% CO_2 in a humidified chamber for a minimum of 72 h before experiments. Cells were

seeded on 13 mm round glass coverslips (Paul Marienfeld 0111530). The coverslips were pretreated with 65% nitric acid for three days, washed with distilled water, 70% ethanol and 100% ethanol thrice each for 30 minutes with gentle rocking and then dried in a cell culture hood overnight under UV. For cell attachment, the treated coverslips were coated with laminin (25 μg/mL in PBS; Sigma L2020) at 37 °C for 1 h, washed thrice with PBS, and then placed at the bottom of a 24-well plate for cell seeding. For all experiments, cells were cultured in RPMI 1640 differentiation media containing 1% HI-HS.

Quantifying cell surface incorporation of PGMs

PC12 cells were harvested and functionalized with either **DPPE-$\{Z_U\}_{12}$-B** or **DPPE-$\{Z\}_{12}$-B** as described above. After incubation, the cells were centrifuged and rinsed with fresh differentiation medium.

For confocal imaging, the cells were then incubated for 30 min at 4 °C in anti-biotin Alexa Fluor 488 (1:300 dilution in PBS/4% FBS; Jackson Immunoresearch 200-542-211) and rinsed again in PBS/4% FBS. The cells were re-suspended in PBS/4% FBS and confocal images were taken with a Carl Zeiss LSM 5 DUO microscope at 20x and 100x magnification by mounting the cell suspension on a microscope slide (Fig. 4B).

For time-course quantification of GAG mimetic incorporation, the cells were seeded onto wells with laminin-coated coverslips in differentiation media. For each time point, cells were harvested by titration and rinsed with PBS/4% FBS. The cells were then incubated with anti-biotin Alexa Fluor 488 as described above and rinsed with PBS (100 μl). 10 μl of cell suspension was removed for cell quantification with an automated cell counter (Bio-Rad TC20). The remaining cells were lysed with cell culture lysis reagent (Promega

#E1531), and the cell lysate transferred to a 96-well plate. Fluorescence was then quantified with a microplate reader (Tecan Infinite M200 Pro, Excitation/Emission: 480/525 nm). Readings were normalized by dividing the fluorescence reading by the cell count and subtracting background signal from non-functionalized cells. Data was plotted with Microsoft Excel and fitted to an exponential decay curve via sum of squared error minimization (Fig. 4B).

Neurite outgrowth assay.

PC12 cells were first harvested and incubated in (i, vii and viii) differentiation media or differentiation media supplemented with 30 μM of (ii) **DPPE-{Z_U}$_{12}$**, (iii) **DPPE-{Z}$_{12}$**, (iv) **DPPE-12-{Z_U}$_{12}$**, (v and ix) **DPPE-12-{Z}$_{12}$**, or (vi) 1 mM of 4-pentyne-1, 2-disulfate for 2 h. After incubation, the cells were centrifuged and rinsed twice with fresh differentiation medium and then seeded onto laminin-coated coverslips at a density of 100 cells/mm^2. After allowing the cells to attach for 1 h at 37 °C, the medium was replaced with fresh differentiation medium supplemented with (i to viii) 200 ng/mL GDNF and 1 μg/mL GFRα1. For vii and viii, **Ac-{Z}$_{12}$** was further added to the supplemented medium to a final concentration of (vii) 10 μM or (viii) 20 μM. For ix, the media was replaced with differentiation medium supplemented with 1 μg/mL of GFRα1 but no GDNF. After 72 h, the cells were fixed with 4% paraformaldehyde solution (Tokyo Chemical Industry 30525-89-4 in PBS) for 15 minutes at room temperature and then rinsed with PBS. Bright-field images were taken using an Olympus IX71 Inverted Microscope at 20x magnification under phase contrast. For each condition, 400 – 500 randomly selected single cells were counted. The percentage of neurite-bearing cells was

determined by counting the number of cells with neurites longer than the cell body. Experiments were repeated three times and done in duplicate each time (Fig. 4C–4D).

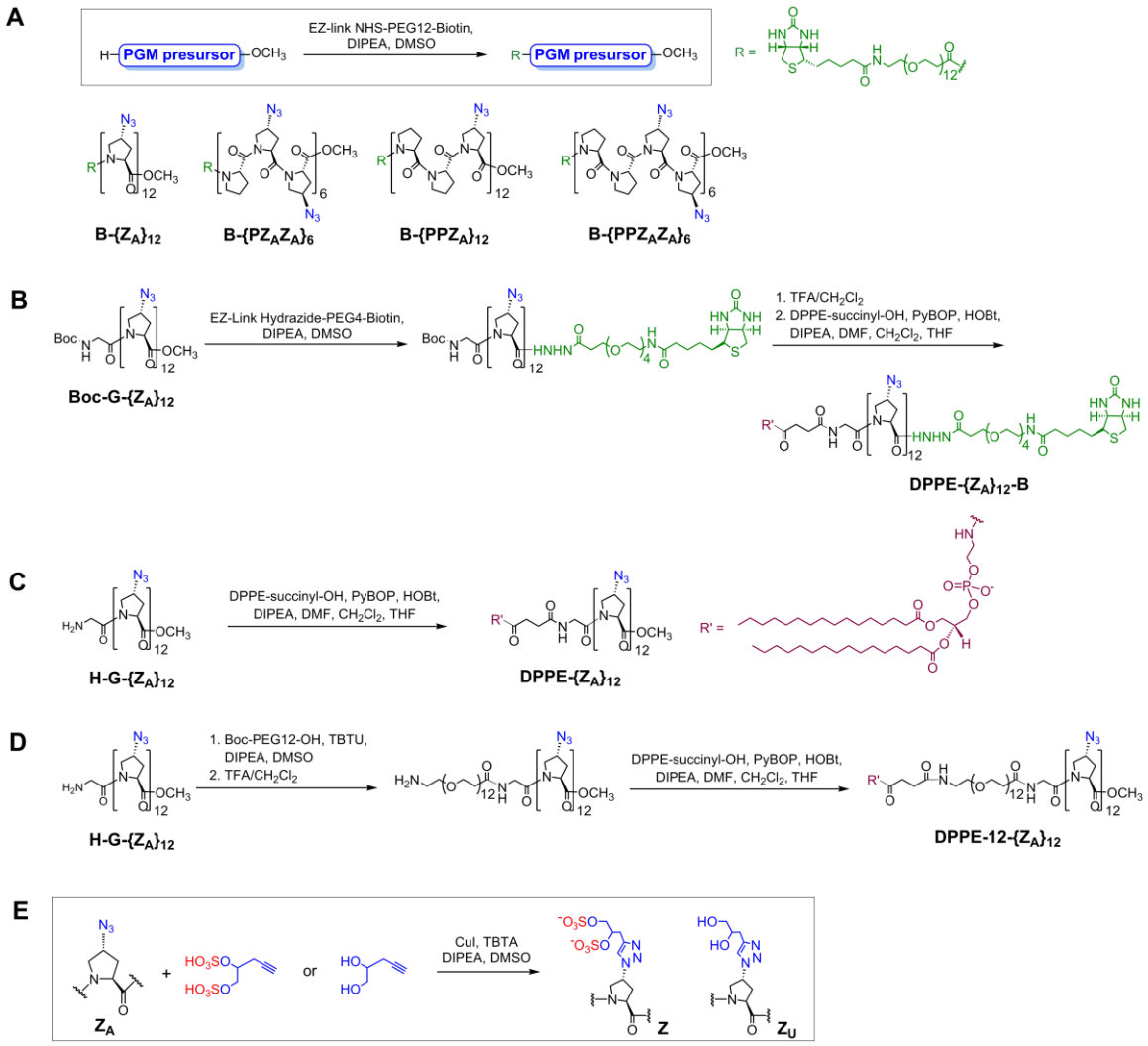

Fig. S1 (A) Structures of PGM precursors **B-{Z_A}$_{12}$**, **B-{PZ_AZ_A}$_6$**, **B-{PPZ_A}$_{12}$** and **B-{PPZ_AZ_A}$_6$**, all of which bear a total of 12 {Z_A} units. (B) Synthesis of **DPPE-{Z_A}$_{12}$-B**. (C) Synthesis of **DPPE-{Z_A}$_{12}$**. (D) Synthesis of **DPPE-12-{Z_A}$_{12}$**. (E) Click reaction for the synthesis of PGMs. **B-{Z}$_{12}$**, **B-{PZZ}$_6$**, **B-{PPZ}$_{12}$**, **B-{PPZZ}$_6$**, **DPPE-{Z_U}$_{12}$**, **DPPE-{Z}$_{12}$**, **DPPE-12-{Z_U}$_{12}$**, **DPPE-12-{Z}$_{12}$**, **DPPE-{Z_U}$_{12}$-B** and **DPPE-{Z}$_{12}$-B**, all of which bear a total of 12 {Z} units.

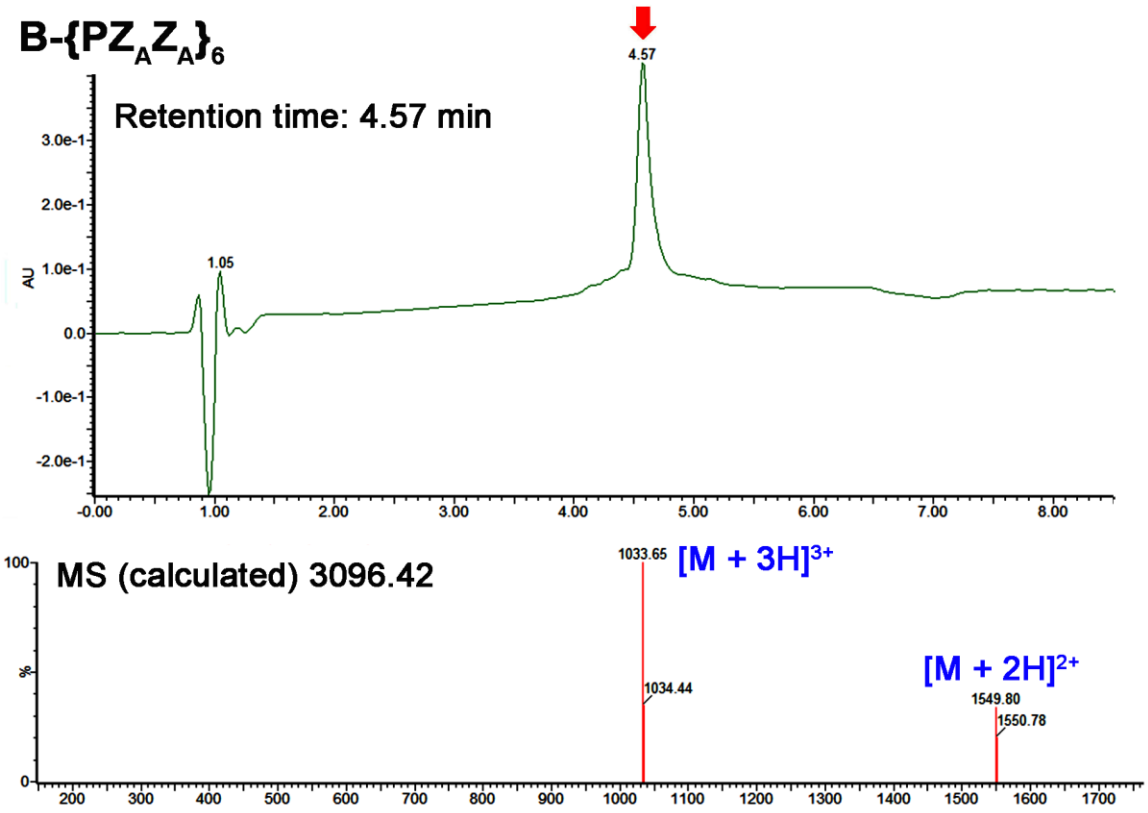

Fig. S2 Analytical HPLC traces (top) and ESI mass data (bottom) of **B-{PZ$_A$Z$_A$}$_6$**.

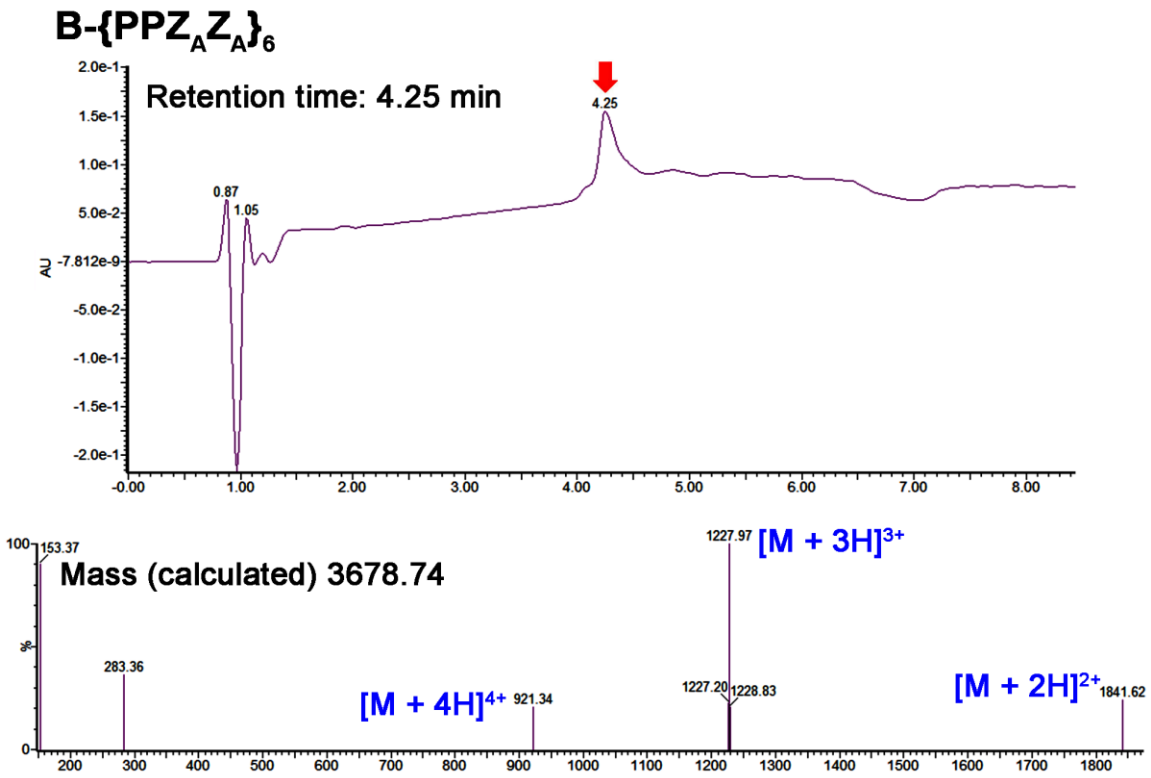

Fig. S3 Analytical HPLC traces (top) and ESI mass data (bottom) of **B-{PPZ$_A$Z$_A$}$_6$**.

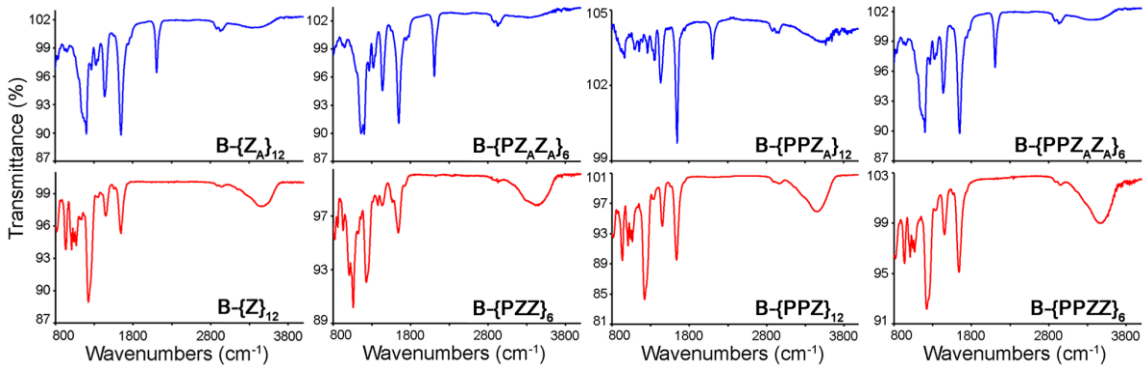

Fig. S4 FT-IR spectra of (blue) biotinylated PGM precursors **B-{Z_A}$_{12}$**, **B-{PZ_AZ_A}$_6$**, **B-{PPZ_A}$_{12}$** and **B-{PPZ_AZ_A}$_6$**, and (red) biotinylated, sulfated PGMs **B-{Z}$_{12}$**, **B-{PZZ}$_6$**, **B-{PPZ}$_{12}$** and **B-{PPZZ}$_6$**.

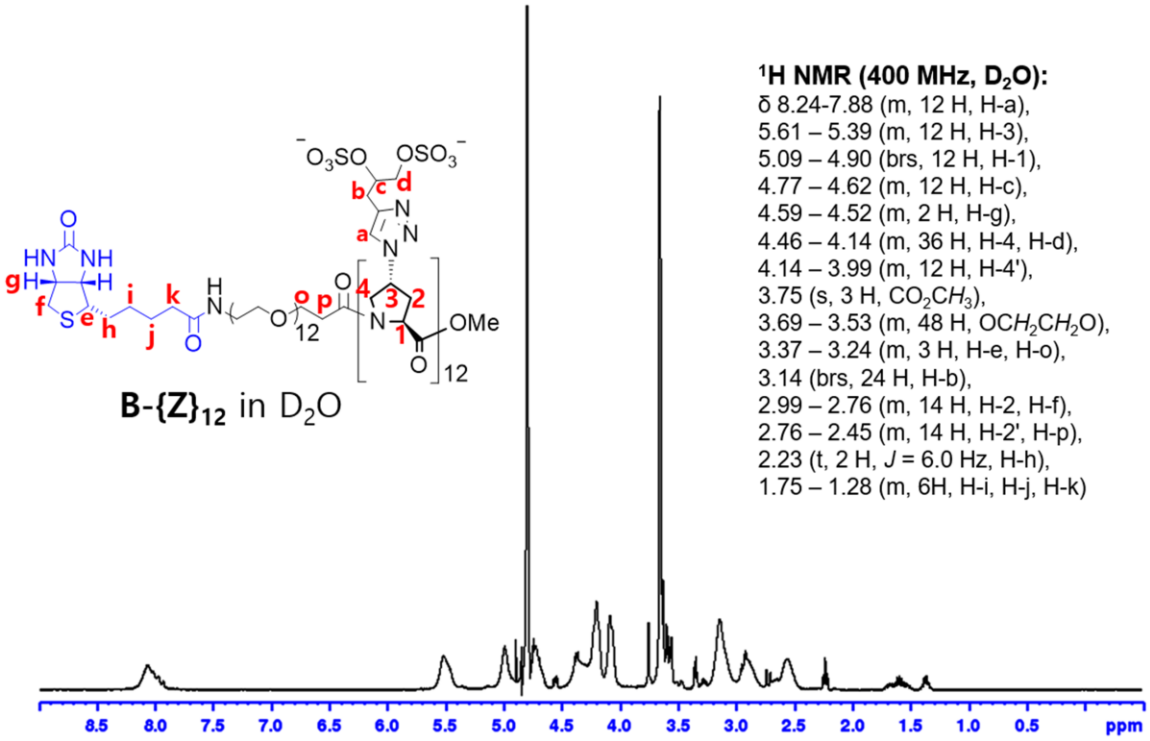

Fig. S5 ^{1}H NMR spectra of **B-{Z}$_{12}$**.

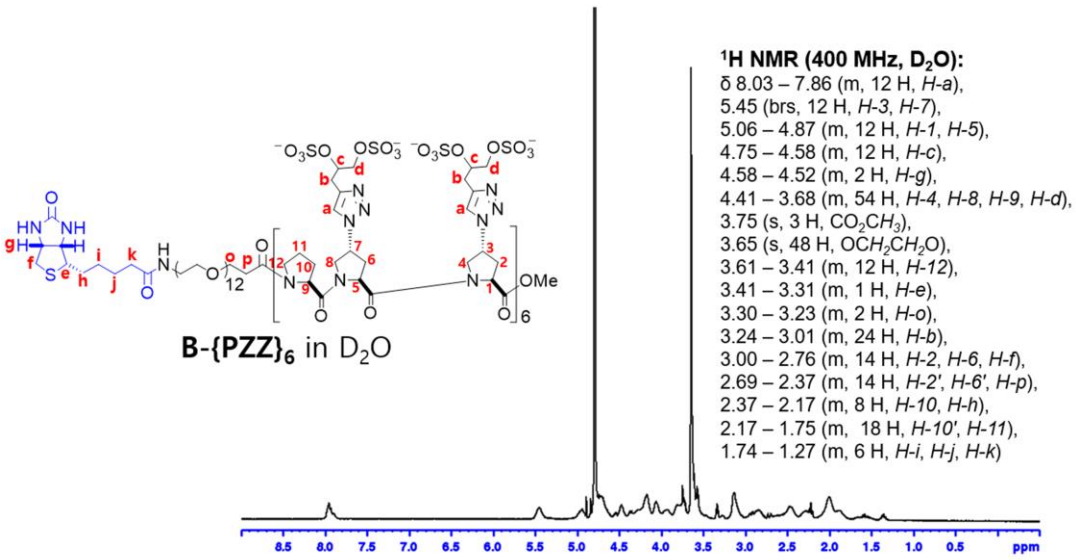

Fig. S6 ^{1}H NMR spectra of **B-{PZZ}$_6$**.

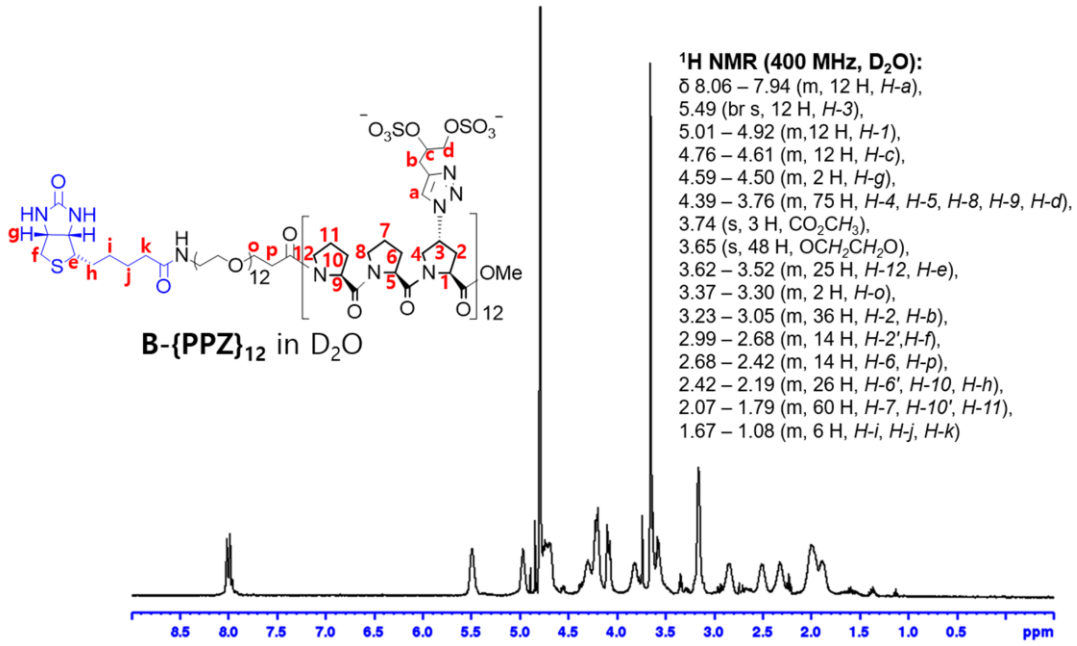

Fig. S7 ^{1}H NMR spectra of **B-{PPZ}$_{12}$**.

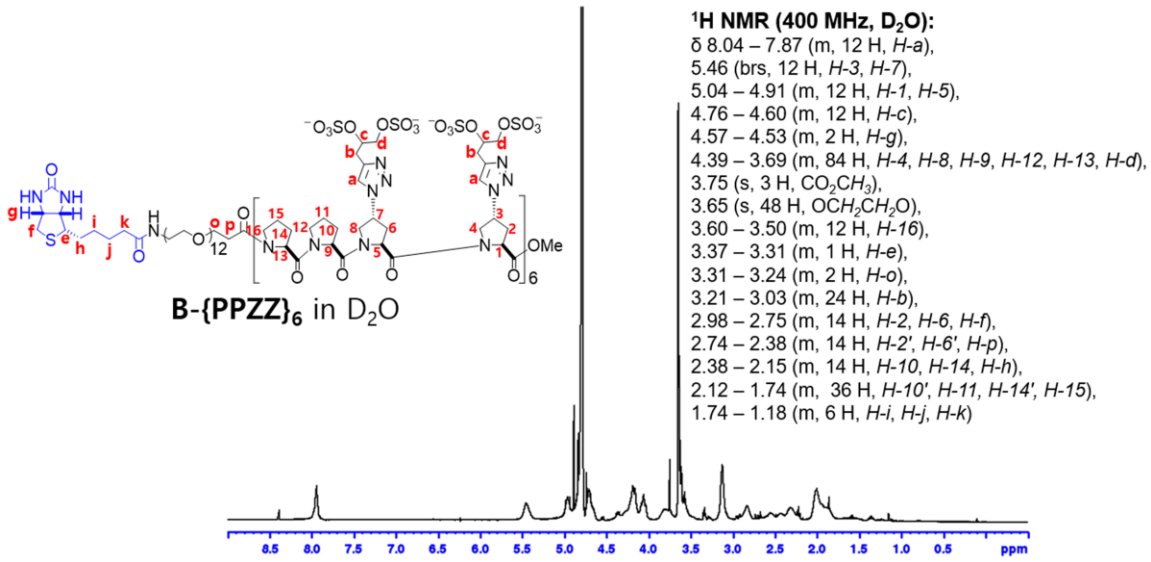

Fig. S8 ^{1}H NMR spectra of **B-{PPZZ}$_6$**.

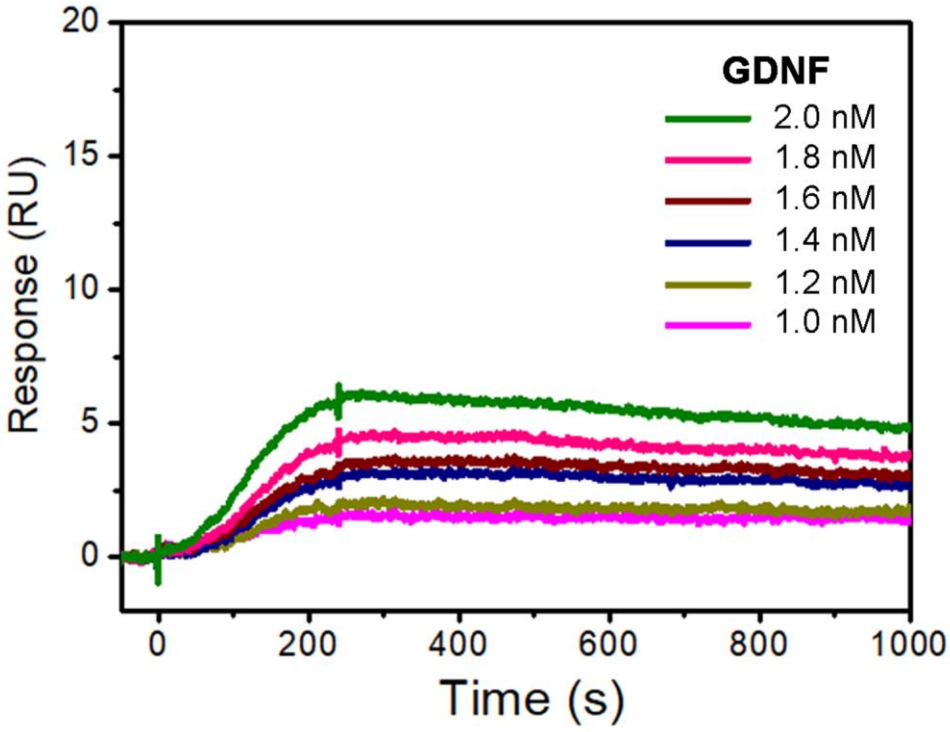

Fig. S9 SPR sensorgram for GDNF binding to heparan sulfate.

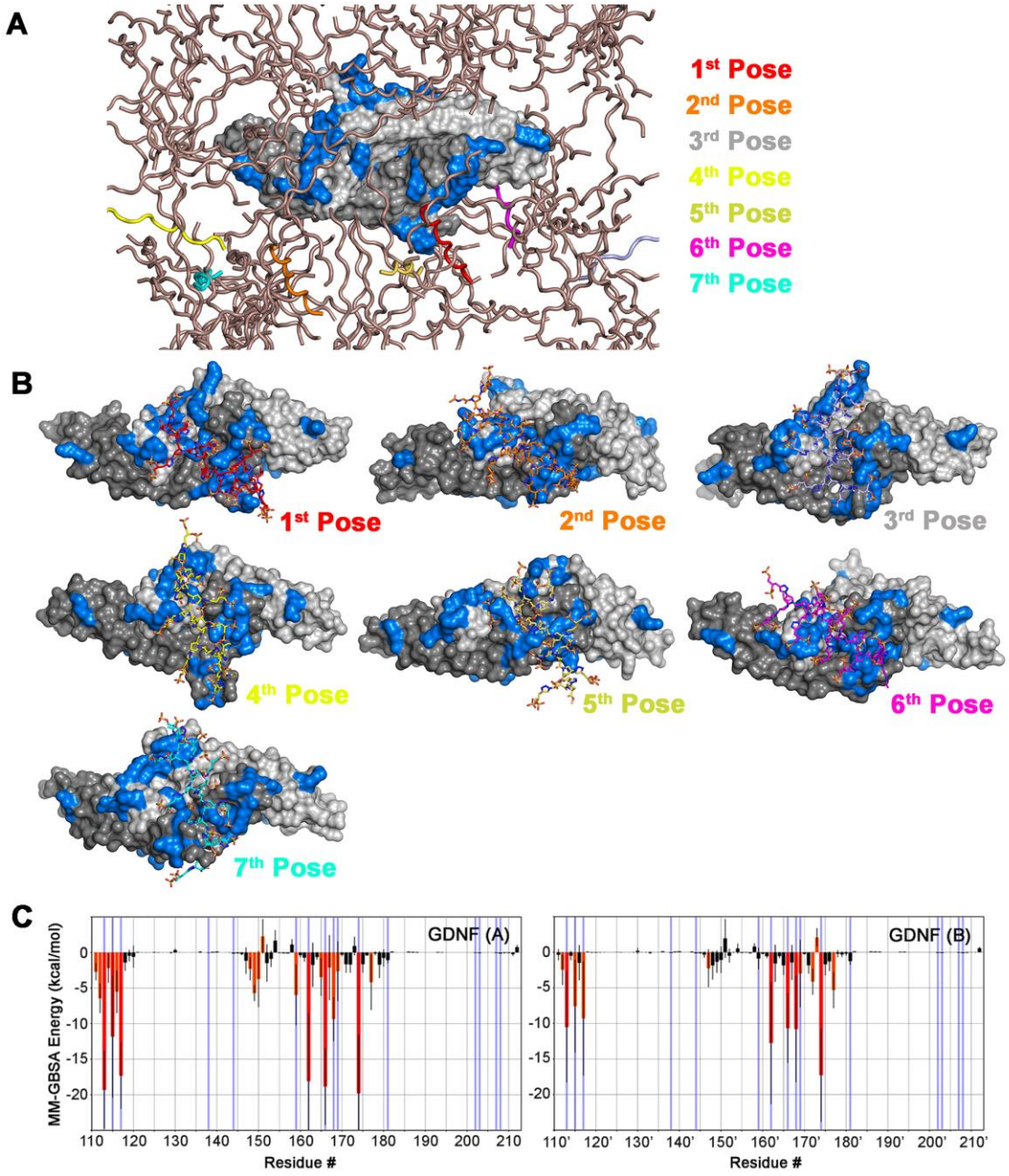

Fig. S10 (A) 200 independent starting geometries showing the initial random placement of $\{Z\}_{12}$ around human GDNF dimer at the center of a 7x7x7 nm^3 cubic box. $\{Z\}_{12}$ is shown as cartoon representation. (B) Human GDNF dimer and the top seven final poses of $\{Z\}_{12}$ as ranked by MM-GBSA analyses after 10 ns of implicit solvent molecular dynamics simulations, run with pmemd using igb=5, mbondi2 radii and a salt concentration of 0.15 M. Blue color denotes basic amino acid residues. (C) Decomposition of average MM-GBSA interaction energies along individual residues on the GDNF dimer bound to top seven final poses of $\{Z\}_{12}$.

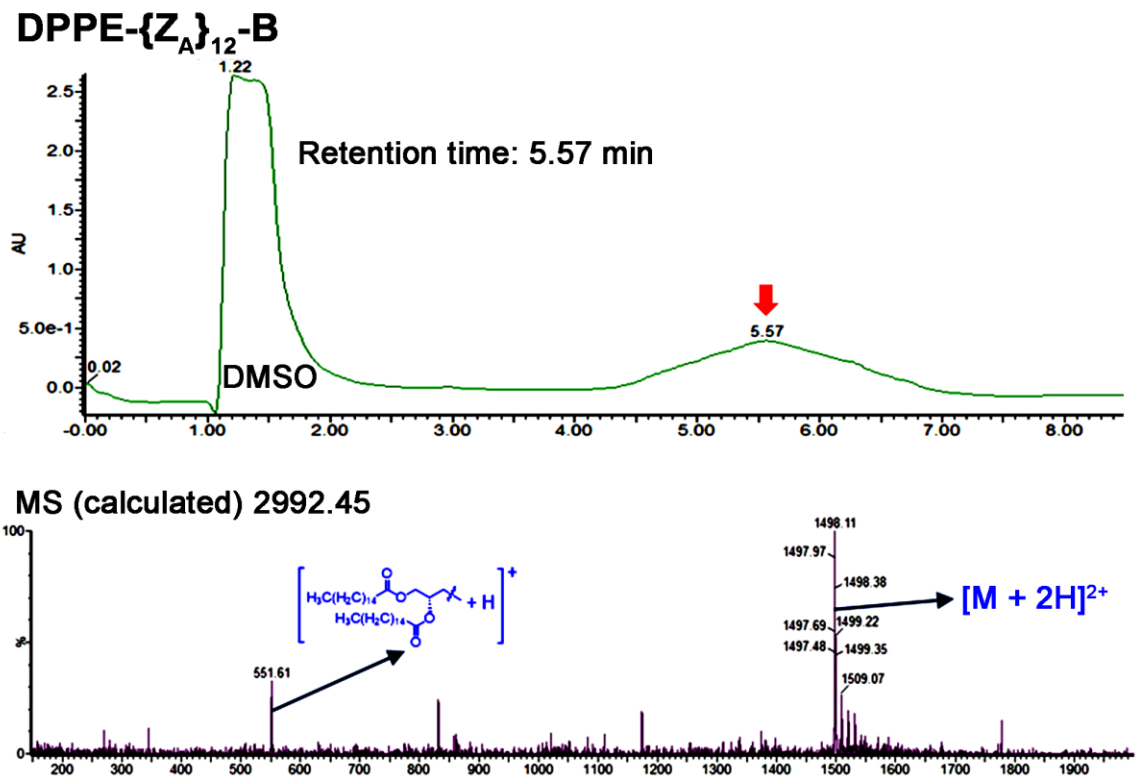

Fig. S11 Analytical HPLC traces (top) and ESI mass data (bottom) of **DPPE-{Z_A}$_{12}$-B**.

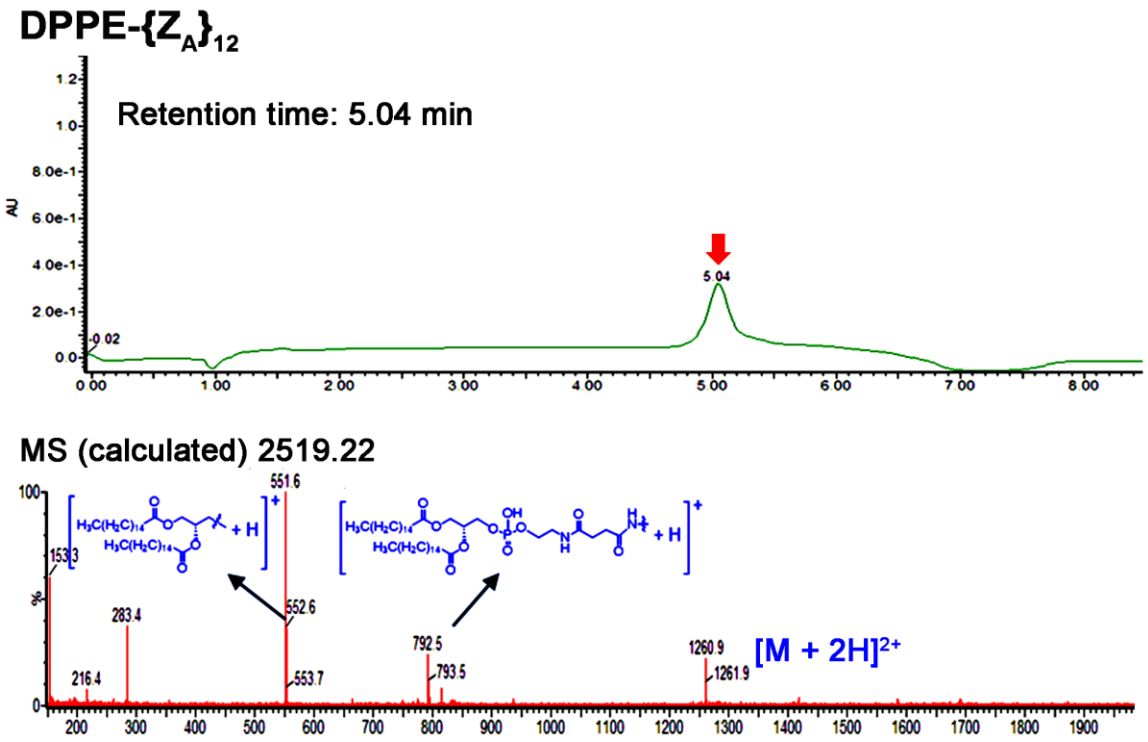

Fig. S12 Analytical HPLC traces (top) and ESI mass data (bottom) of **DPPE-{Z_A}$_{12}$**.

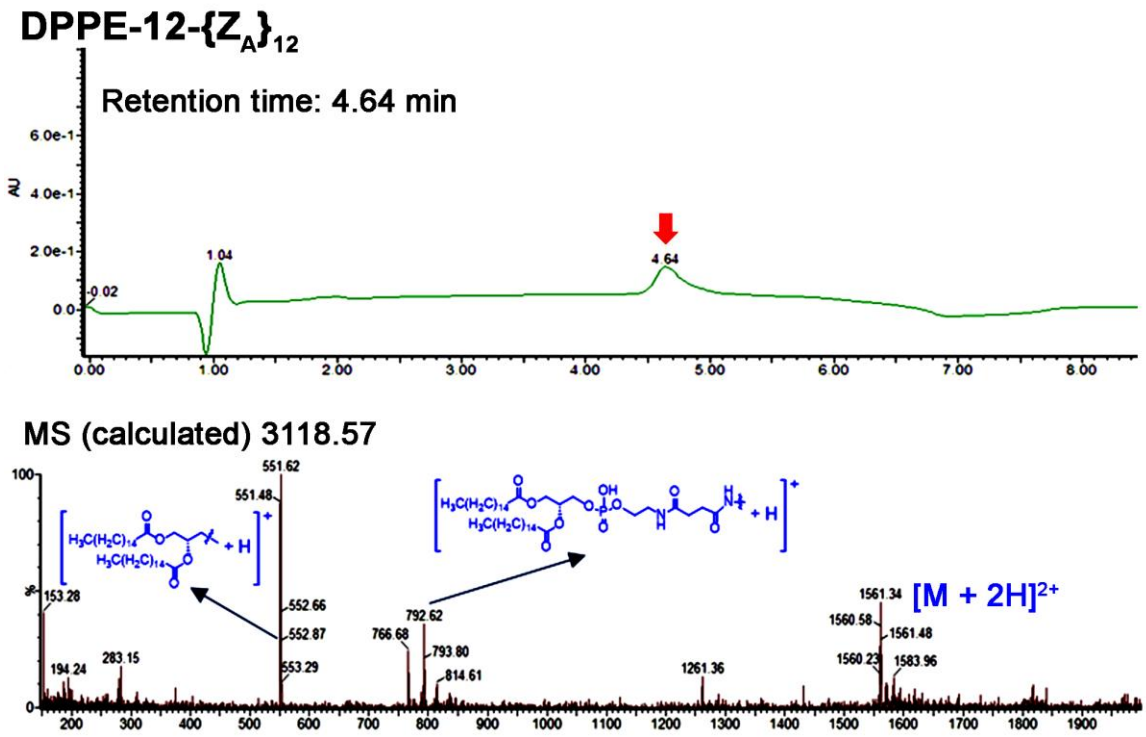

Fig. S13 Analytical HPLC traces (top) and ESI mass data (bottom) of **DPPE-12-{Z_A}$_{12}$**.

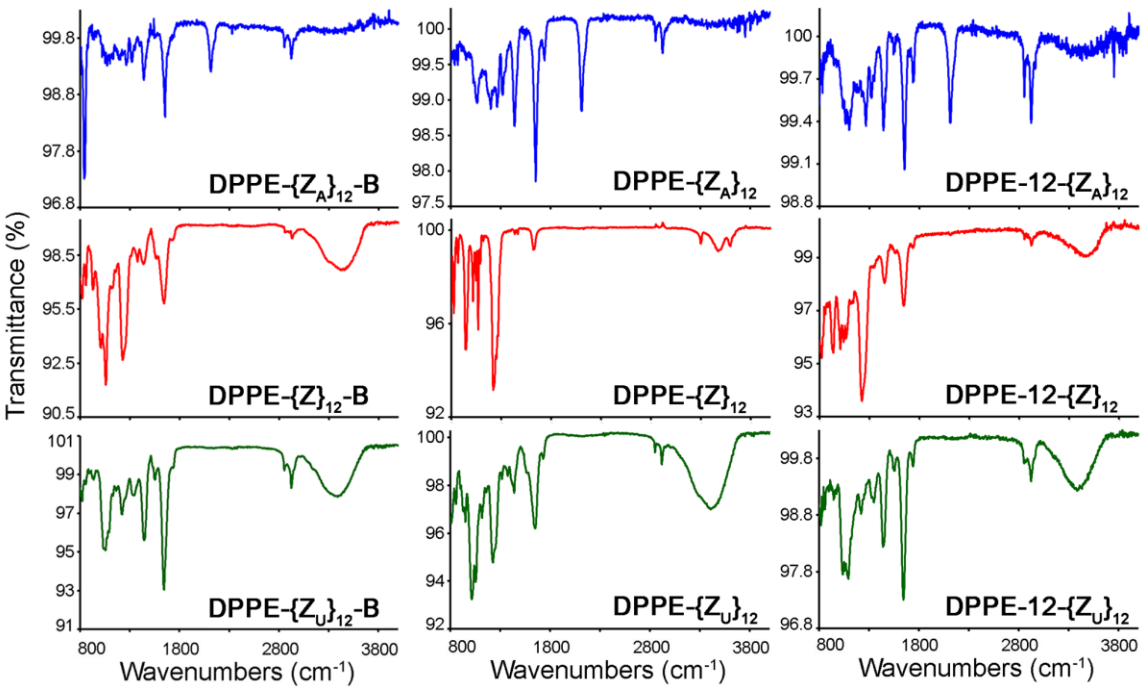

Fig. S14 FT-IR spectra of (blue) DPPE-anchored PGM precursors **DPPE-{Z_A}$_{12}$-B**, **DPPE-{Z_A}$_{12}$** and **DPPE-12-{Z_A}$_{12}$**, (red) DPPE-anchored, sulfated PGMs **DPPE-{Z}$_{12}$-B**, **DPPE-{Z}$_{12}$** and **DPPE-12-{Z}$_{12}$** and (green) unsulfated, dihydroxyl variants of DPPE-anchored PGMs **DPPE-{Z_U}$_{12}$-B**, **DPPE-{Z_U}$_{12}$** and **DPPE-12-{Z_U}$_{12}$**.

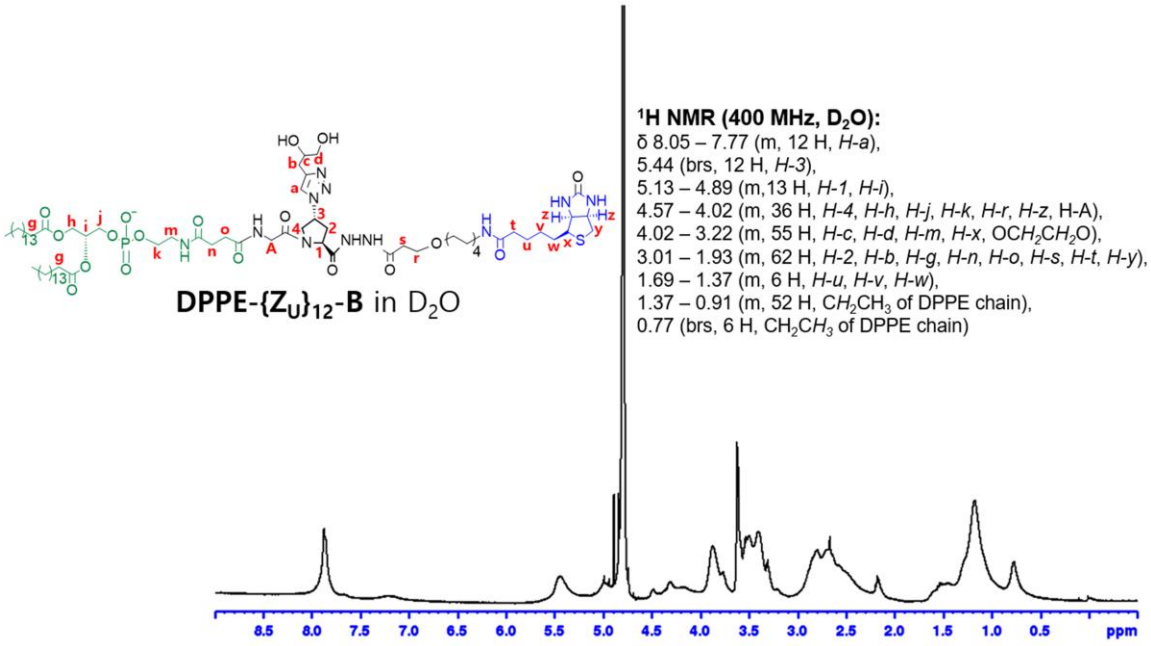

Fig. S15 ^{1}H NMR spectra of **DPPE-{Z_U}$_{12}$-B**.

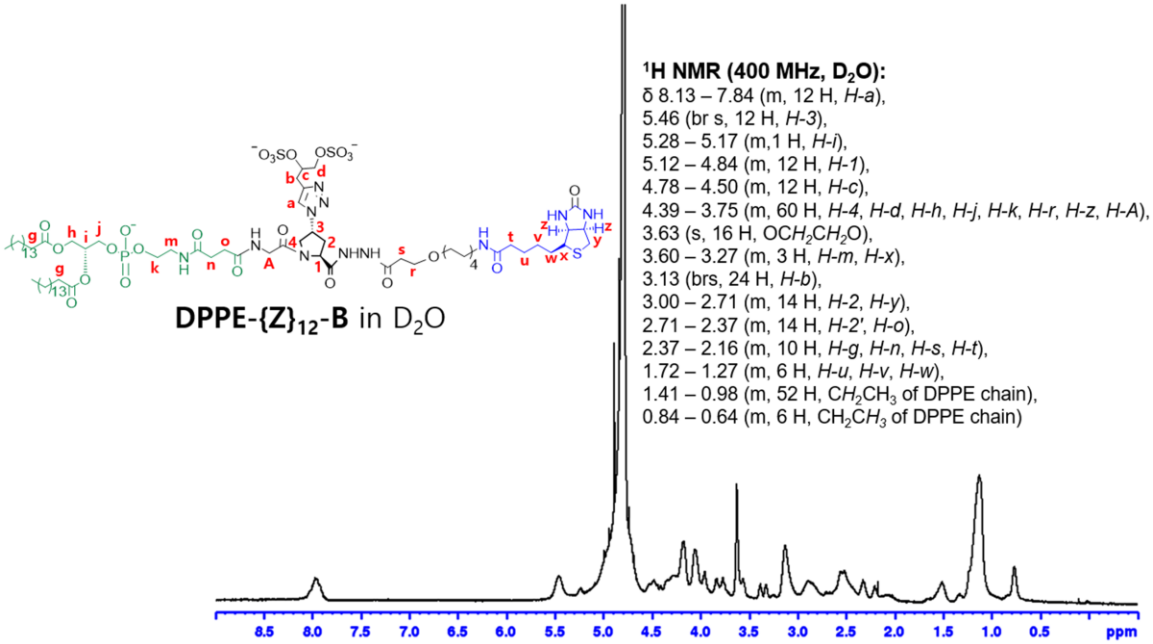

Fig. S16 ^{1}H NMR spectra of **DPPE-{Z}$_{12}$-B**.

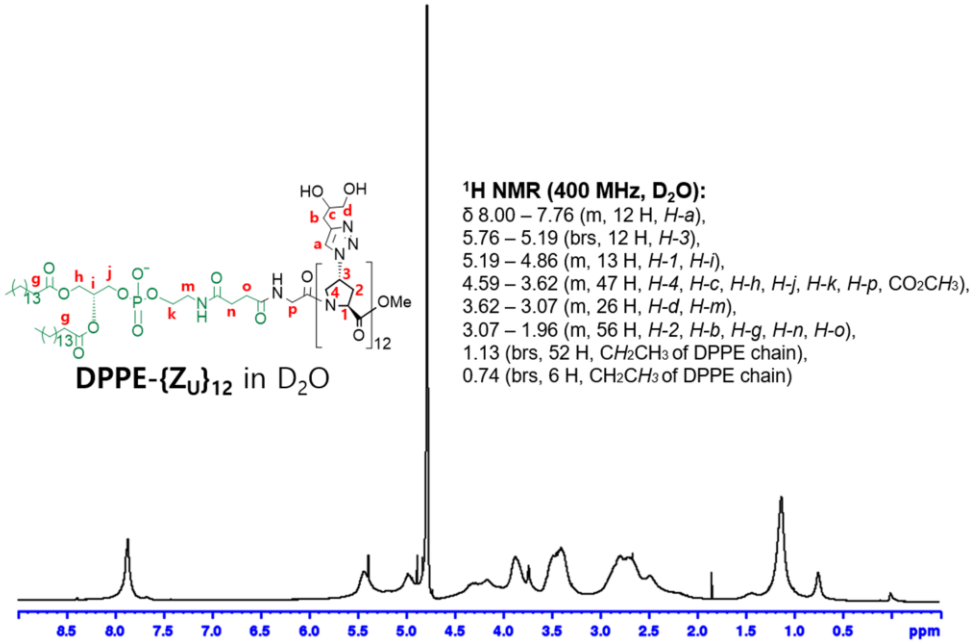

Fig. S17 ^{1}H NMR spectra of **DPPE-{Z_U}$_{12}$**.

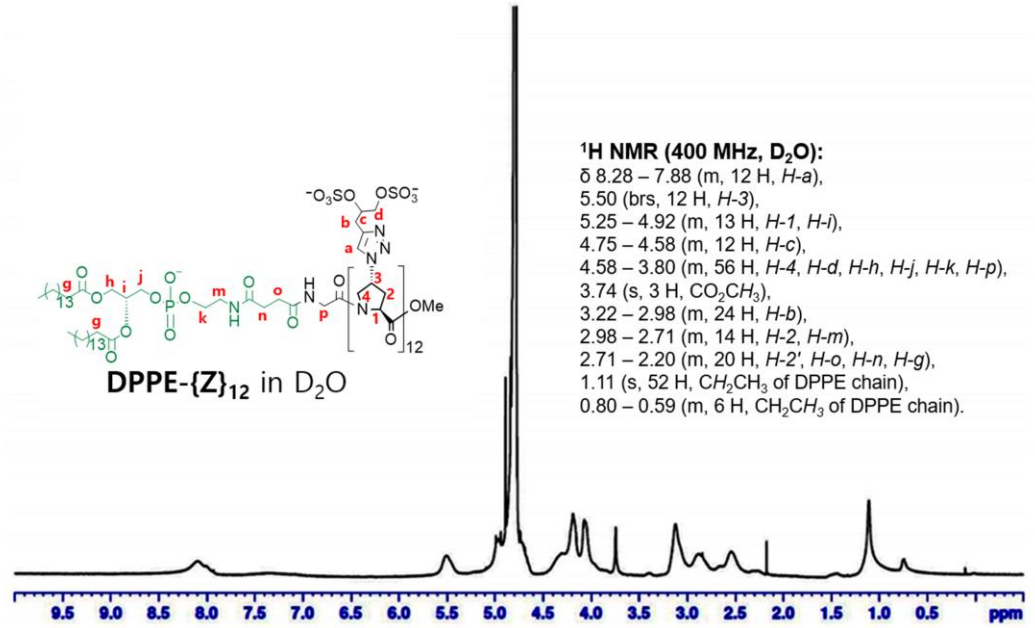

Fig. S18 ^{1}H NMR spectra of **DPPE-{Z}$_{12}$**.

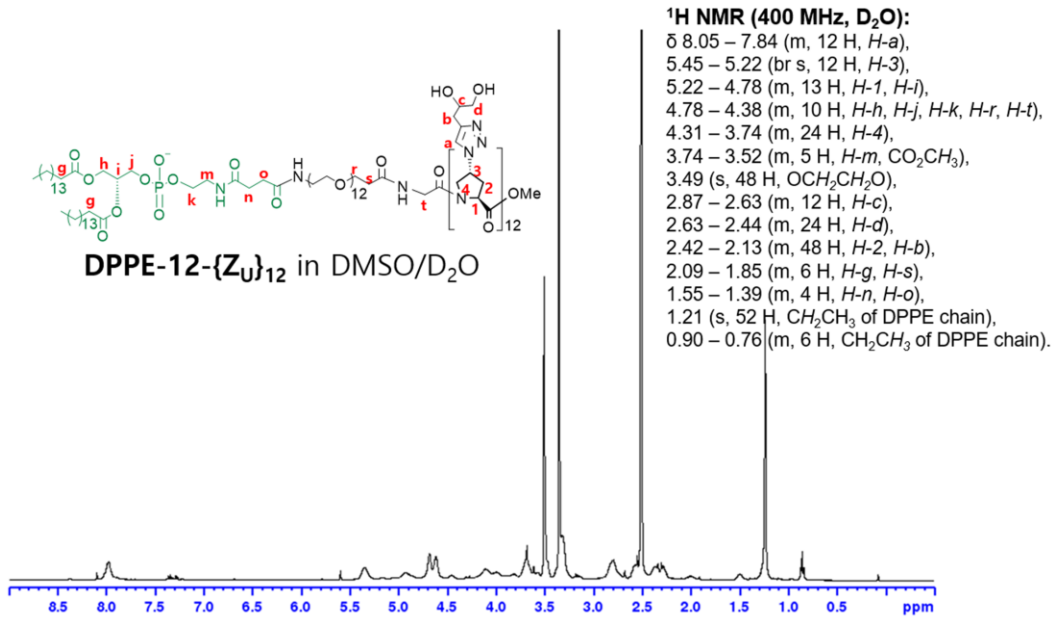

Fig. S19 ^{1}H NMR spectra of **DPPE-12-{Z_U}$_{12}$**.

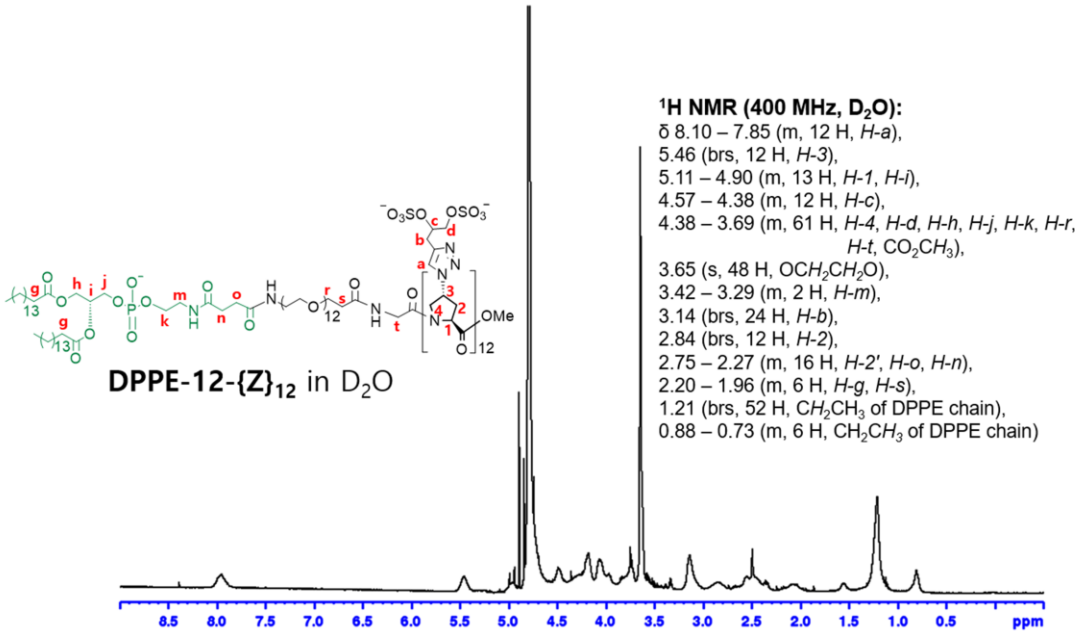

Fig. S20 ^{1}H NMR spectra of **DPPE-12-{Z}$_{12}$**.

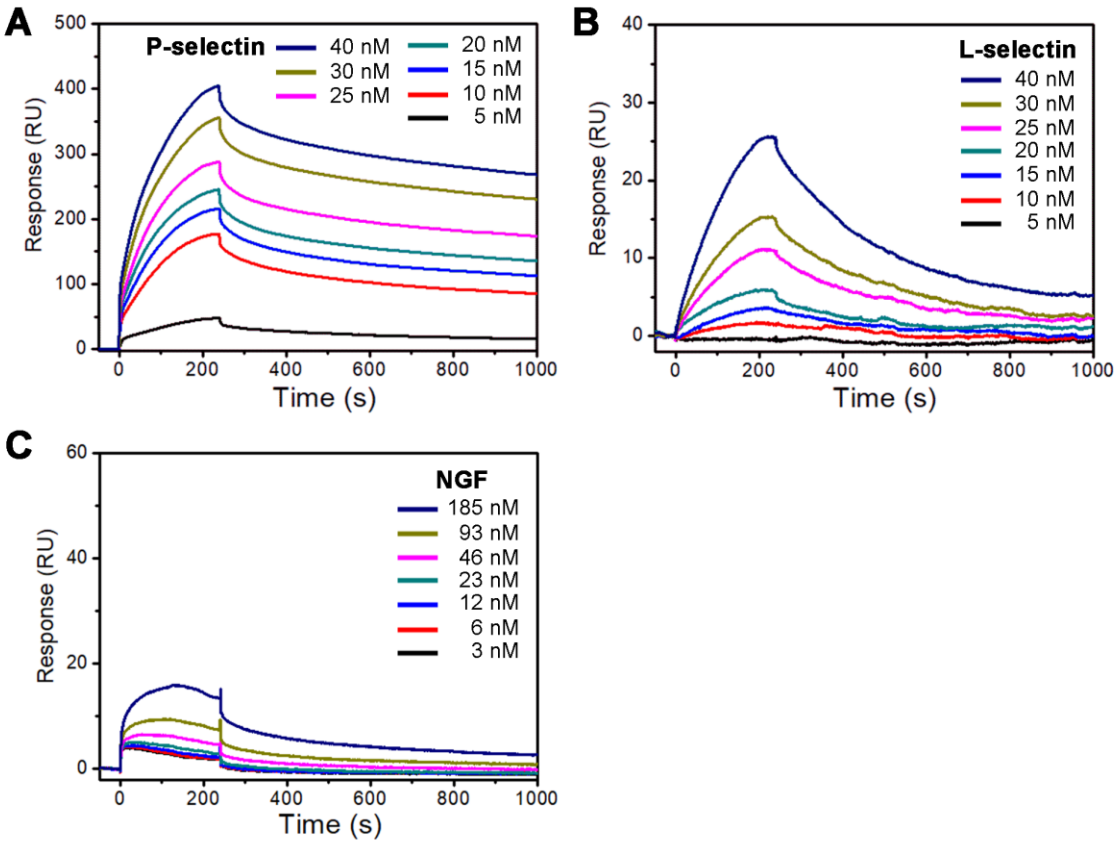

Fig. S21 SPR sensorgrams for (A) P-selectin binding to **{Z}$_{12}$**, (B) L-selectin binding to **{Z}$_{12}$** and (C) NGF binding to **{Z}$_{12}$**.

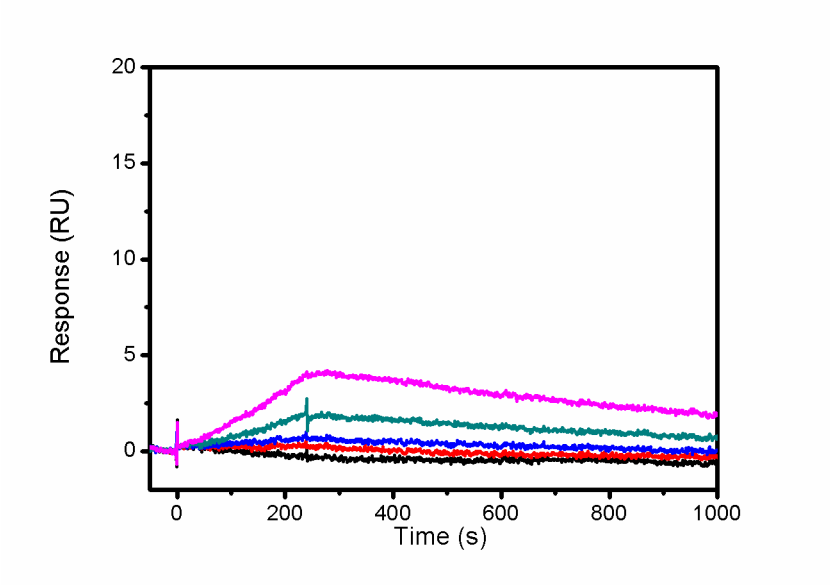

Fig. S22 SPR sensorgram for GFRα1 binding to **B-{Z}$_{12}$**.

Table S1. Calculated equilibrium binding constants of proteins with **B-{Z}$_{12}$**, **B-{PZZ}$_{6}$**, **B-{PPZ}$_{12}$**, **B-{PPZZ}$_{6}$** and natural HS.

	k_a ($M^{-1}S^{-1}$)	k_d (S^{-1})	K_D (M)[a]
GDNF			
B-{Z}$_{12}$	6.42 (± 0.28) x 10^{5}	2.12 (± 0.07) x 10^{-3}	3.30 x 10^{-9}
B-{PZZ}$_{6}$	1.94 (± 0.11) x 10^{5}	2.40 (± 0.05) x 10^{-3}	1.24 x 10^{-8}
B-{PPZ}$_{12}$	ND[b]	ND[b]	ND[b]
B-{PPZZ}$_{6}$	ND[b]	ND[b]	ND[b]
Natural HS	7.13 (± 2.61) x 10^{5}	5.84 (± 1.32) x 10^{-2}	8.19 x 10^{-8}
GFRα1			
B-{Z}$_{12}$	4.26 (± 0.90) x 10^{5}	4.9 (± 1.7) x 10^{-2}	1.16 x 10^{-7}
P-selectin			
B-{Z}$_{12}$	6.25 (± 0.11) x 10^{4}	3.74 (± 0.04) x 10^{-4}	5.99 x 10^{-9}
L-selectin			
B-{Z}$_{12}$	1.66 (± 0.09) x 10^{3}	2.55 (± 0.04) x 10^{-3}	1.54 x 10^{-6}
NGF			
B-{Z}$_{12}$	9.29 (± 0.46) x 10^{2}	8.10 (± 0.10) x 10^{-4}	8.72 x 10^{-6}

[a] K_D values were obtained independently from each k_a and k_d value using Biacore T100 evaluation software v 2.0.4.

[b] ND = not determined. The exact kinetic parameters were not calculated due to a decrease in response after reaching equilibrium in the association phase.

Supplementary References

1. P. Liu, L. Chen, J. K. C. Toh, Y. L. Ang, J.-E. Jee, J. Lim, S. S. Lee and S.-G. Lee, *Chem. Sci.*, 2015, **6**, 450–456.
2. D. A. Case, T. E. Cheatham, T. Darden, H. Gohlke, R. Luo, K. M. Merz, A. Onufriev, C. Simmerling, B. Wang and R. J. Woods, *J. Comput. Chem.*, 2005, **26**, 1668–1688.
3. J. A. Maier, C. Martinez, K. Kasavajhala, L. Wickstrom, K. E. Hauser and C. Simmerling, *J. Chem. Theory Comput.* 2015, **11**, 3696–3713.
4. T. C. Lim, S. Cai, R. G. Huber, P. J. Bond, P. X. S. Chia, S. L. Khou, S. Gao, S. S. Lee and S.-G. Lee, *Chem. Sci.*, 2018, **9**, 7940–7947.
5. V. Parkash, V.-M. Leppänen, H. Virtanen, J. M. Jurvansuu, M. M. Bespalov, Y. A. Sidorova, P. Runeberg-Roos, M. Saarma and A. Goldman, *J. Biol. Chem.* 2008, **283**, 35164–35172.
6. M. J. Abraham, T. Murtola, R. Schulz, S. Páll, J. C. Smith, B. Hess and E. Lindah, *SoftwareX*, 2015, **1–2**, 19–25.
7. S. A. Samsonov, J. P. Gehrcke and M. T. Pisabarro, *J. Chem. Inf. Model.*, 2014, **54**, 582–592.
8. A. W. Götz, M. J. Williamson, D. Xu, D. Poole, S. Le Grand and R. C. Walker, *J. Chem. Theory Comput.*, 2012, **8**, 1542–1555.
9. A. Onufriev, D. Bashford and D. A. Case, *Proteins Struct. Funct. Genet.*, 2004, **55**, 383–394.
10. S. Genheden and U. Ryde, *Expert Opin. Drug Discov.*, 2015, **10**, 449–461.